DESY-22-025

Back-to-back azimuthal correlations in Z+jet events at high transverse momentum in the TMD parton branching method at next-to-leading order

H. Yang[1,2], A. Bermudez Martinez[2], L.I. Estevez Banos[2], F. Hautmann[3,4,5], H. Jung[2], M. Mendizabal[2], K. Moral Figueroa[6], S. Prestel[7], S. Taheri Monfared[2], A.M. van Kampen[4], Q. Wang[2,1], and K. Wichmann[2]

[1]School of Physics, Peking University
[2]Deutsches Elektronen-Synchrotron DESY, Germany
[3]CERN, Theoretical Physics Department, Geneva
[4]Elementary Particle Physics, University of Antwerp, Belgium
[5]University of Oxford, UK
[6]University of Edinburgh, UK
[7]Department of Astronomy and Theoretical Physics, Lund University, Sweden

June 21, 2022

Abstract

Azimuthal correlations in Z+jet production at large transverse momenta are computed by matching Parton - Branching (PB) TMD parton distributions and showers with NLO calculations via MCatNLO. The predictions are compared with those for dijet production in the same kinematic range. The azimuthal correlations $\Delta\phi$ between the Z boson and the leading jet are steeper compared to those in dijet production at transverse momenta $\mathcal{O}(100)$ GeV, while they become similar for very high transverse momenta $\mathcal{O}(1000)$ GeV. The different patterns of Z+jet and dijet azimuthal correlations can be used to search for potential *factorization - breaking* effects in the back-to-back region, which depend on the different color and spin structure of the final states and their interferences with the initial states. In order to investigate these effects experimentally, we propose to measure the ratio of the distributions in $\Delta\phi$ for Z+jet- and multijet production at low and at high transverse momenta, and compare the results to predictions obtained assuming factorization. We examine the role of theoretical uncertainties by performing variations of the factorization scale, renormalization scale and matching scale. In particular, we present a comparative study of matching scale uncertainties in the cases of PB-TMD and collinear parton showers.

1 Introduction

The description of the cross section of high p_{T} jets in association with a Z boson at high p_{T} in proton-proton (pp) collisions is an important test of predictions obtained in Quantum Chromodynamics (QCD), and provides an important background to Higgs boson studies and to new physics searches. At leading order in the strong coupling α_{s}, the azimuthal angle $\Delta\phi$ between the Z boson and the jet is $\Delta\phi = \pi$, and a deviation from this back-to-back scenario is a measure of higher order radiation. In multijet events the azimuthal correlation between two jets has been measured at the LHC by ATLAS and CMS [1–5]. The production of Z bosons associated with jets has been measured at lower energies, by CDF and D0 in proton-antiproton collisions at a center-of-mass energy $\sqrt{s} = 1.96$ TeV [6,7]. At the LHC the ATLAS and CMS collaborations have published measurements in pp collisions at a center-of-mass energy $\sqrt{s} = 7$ TeV [8–10], 8 TeV [11] and 13 TeV [12,13]. The azimuthal correlation between Z bosons and jets has been measured at 8 TeV [11] and 13 TeV [13]. However, all the measurements of azimuthal correlations were performed at rather low transverse momenta of the Z boson and the jets ($p_{\mathrm{T}} < \mathcal{O}(100)$ GeV), where multiparton emissions are significant and next-to-leading-order (NLO) calculations of Z+jet are not sufficient to describe the measurement. Theoretical predictions for the low $p_{\mathrm{T},Z}$ region including soft gluon resummation are given in Refs. [14–17]. With the increase in luminosity at the LHC, it becomes possible to measure Z+jet production in the high p_{T} range, with $p_{\mathrm{T},Z} \gg 100$ GeV. Especially the back-to-back region can be studied in detail, which gives important information on soft gluon resummation and effects of the transverse momenta of the initial partons in the form of transverse momentum dependent (TMD) parton distributions (PDFs).

In a previous publication [18] we have investigated the $\Delta\phi_{12}$ correlation in high-p_{T} dijet events by applying TMD PDFs and parton shower together with NLO calculations of the

hard scattering process. The application of TMD PDFs allows a direct investigation of initial state parton radiation (an overview on TMD PDFs is given in Ref. [19]). While hard perturbative higher order radiation leads to a large azimuthal decorrelation ($\Delta\phi_{12} \ll \pi$), soft multi-gluon emissions, which cannot be described by fixed order calculations, dominate in the region $\Delta\phi_{12} \to \pi$. The region of $\Delta\phi_{12} \to \pi$ is of special interest, since so-called *factorization - breaking* [20–22] effects could become important in the case of colored final states. Multijet production is believed to be sensitive to such effects, as well as vector boson + jet production [23]. In order to investigate factorization - breaking effects, we propose to compare the theoretical description of the azimuthal correlation $\Delta\phi_{12}$ in multijet production with the one in Z+jet production. A theoretical investigation of azimuthal correlations in the back-to-back region in Z+jet events has been also performed in Ref. [24], addressing the issue of *factorization - breaking*.

In this report we compare in detail high-p_{T} dijet and Z+jet production by applying the Parton Branching (PB) formulation of TMD evolution [25,26] together with NLO calculations of the hard scattering process in the MADGRAPH5_AMC@NLO [27] framework. In Ref. [18] these PB TMD PDFs were applied to multijet production at large transverse momenta. We apply the same method to the calculation of Z+jet production. We propose to use the same kinematic region for the high-p_{T} dijet and Z+jet production to allow a direct comparison of the measurements. At large enough p_{T} the mass of the Z-boson becomes negligible, and the different color and spin structure of the final states might allow to observe factorization - breaking effects by comparing the measurements to calculations assuming that factorization holds.

In the following, we describe the basic elements of the Z+jet calculation in Sec. 2. In Sec. 3 we present results for the Z+jet azimuthal correlations and compare them with the multijet case. We summarize in Sec. 4. In an appendix we discuss technical details on the use of MCatNLO+CASCADE3.

2 PB - method and calculation of Z+jet distributions

The PB - formulation of TMD evolution is given in Refs. [25, 26], introducing Sudakov form factors and the soft-gluon resolution scale z_M to separate resolvable and non-resolvable branchings. The evolution equation for PB - TMD parton densities (cf eq.(2.43) in Ref. [26]) is based on an integral formulation of the DGLAP [28–31] evolution equation in terms of Sudakov form factors. By integrating over transverse momenta, the PB-TMD evolution equations coincide with the DGLAP [28–31] evolution equation for $z_M \to 1$, while they coincide with the CMW [32, 33] coherent branching equation for finite, angular-ordered z_M [34].

The NLO PB collinear and TMD parton distribution were obtained in Ref. [35] from QCD fits to precision DIS data from at HERA [36]. Two different sets, PB-NLO-2018-Set 1 and PB-NLO-2018-Set 2, were obtained, with PB-NLO-2018-Set 1 corresponding at collinear level to HERAPDF 2.0 NLO [36]. In PB-NLO-2018-Set 2 the transverse momentum (instead of the evolution scale in Set 1) is used as the scale in the running coupling α_{s} which corresponds

to the angular ordering of soft gluon emissions in the initial-state parton evolution [33, 34, 37, 38]. Since it has been shown for Z - production [39, 40] that Set 2 provides a much better description of experimental measurements, we concentrate here on Set 2 only.

In Fig. 1 we show the TMD PDF distributions for up quarks and gluons at $x = 0.01$ and $\mu = 100$ and 1000 GeVfor PB-NLO-2018-Set 2. The transverse momentum distribution of gluons is broader than that of quarks, due to gluon self-coupling and the different color factors. In Fig. 1 also the uncertainties of the distributions, as obtained from the fit [35], are shown. The differences in the transverse momentum spectra of quarks and gluons will show up in differences in azimuthal correlation distributions.

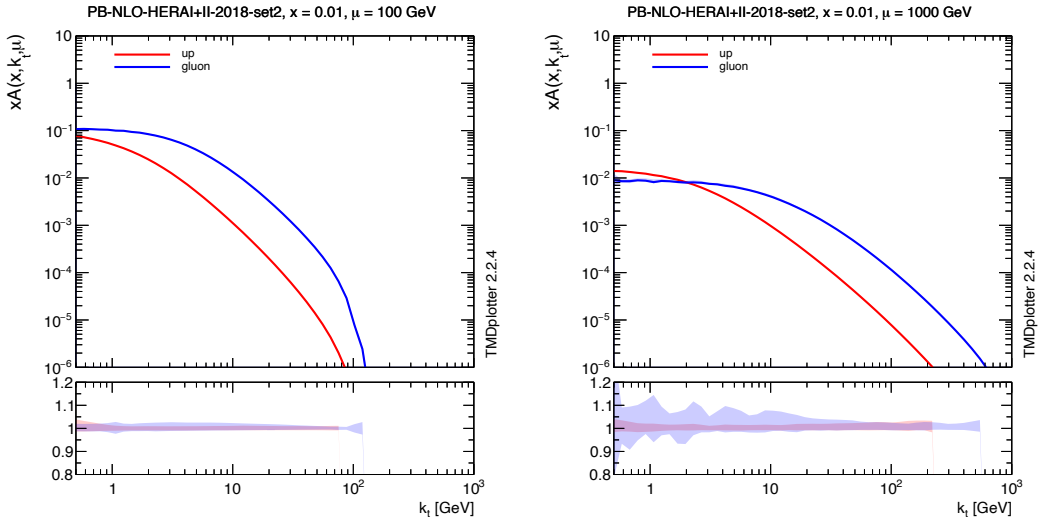

Figure 1: TMD parton density distributions for up quarks and gluons of PB-NLO-2018-Set 2 as a function of k_{T} at $\mu = 100$ and 1000 GeV and $x = 0.01$. In the lower panels show the full uncertainty of the TMD PDFs, as obtained from the fits [35].

The process Z+jet at NLO is calculated with MADGRAPH5_AMC@NLO using the collinear PB-NLO-2018-Set 2, as obtained in Ref. [35] applying $\alpha_{\mathrm{s}}(M_{\mathrm{Z}}) = 0.118$. The matching of NLO matrix elements with PB TMD parton distributions is described in Refs. [40–42]. The extension to multijet production is illustrated in Ref. [18]. Predictions are obtained by processing the MADGRAPH5_AMC@NLO event files in LHE format [43] through CASCADE3 [42] for an inclusion of TMD effects in the initial state and for simulation of the corresponding parton shower (labeled MCatNLO+CAS3 in the following).

Fixed order NLO Z+jet production is calculated with MADGRAPH5_AMC@NLO in a procedure similar to the one applied for dijet production described in [18] (labeled MCatNLO(fNLO)). For the MC@NLO mode, the HERWIG6 [44, 45] subtraction terms are calculated, as they are best suited for the use with PB - parton densities, because both apply the same angular ordering condition. The use HERWIG6 subtraction terms together with

CASCADE3 is justified in appendix Section 5 for final state parton shower as well as initial and final state showers by a comparison of the predictions obtained with CASCADE3 and with HERWIG6. The matching scale μ_m = SCALUP limits the contribution from PB-TMDs and TMD showers.

In the calculations, the factorization and renormalization scales are set to $\mu = \frac{1}{2}\sum_i p_{\mathrm{T},i}$, where the index i runs over all particles in the matrix element final state. This scale is also used in the PB-TMD parton distribution $\mathcal{A}(x, k_{\mathrm{T}}, \mu)$. The scale uncertainties of the predictions are obtained from variations of the scales around the central value in the 7-point scheme avoiding extreme cases of variation.

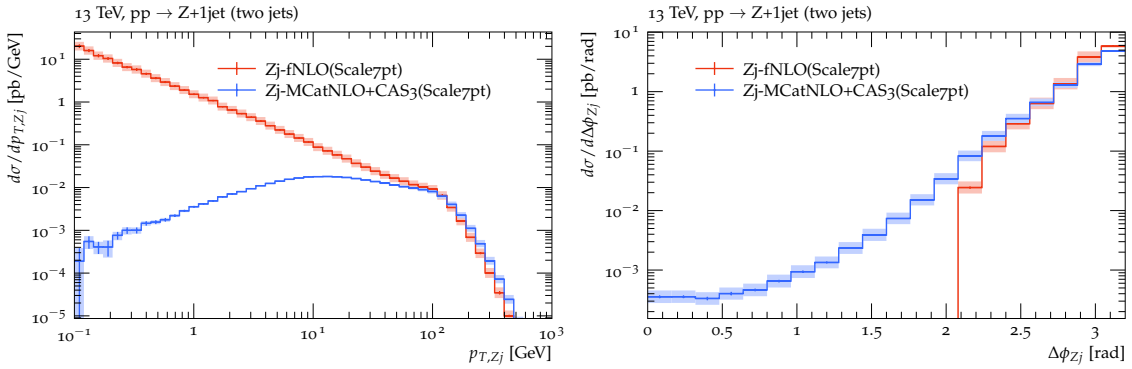

Figure 2: Transverse momentum spectrum of the Z+jet-system $p_{\mathrm{T},Zj}$ (left) and $\Delta\phi_{\mathrm{Zj}}$ distribution (right). The predictions are shown for fixed NLO (MCatNLO(fNLO) and after inclusion of PB-TMDs (MCatNLO+CAS3).

In Fig. 2 we show the distributions of the transverse momentum of the Z+jet system, $p_{\mathrm{T},Zj}$, and the azimuthal correlation in the Z+jet system, $\Delta\phi_{\mathrm{Zj}}$, for a fixed NLO calculation, as well as for the full simulation including PB-TMD PDFs and parton showers. We require a transverse momentum $p_{\mathrm{T}} > 200$ GeV for the Z boson and define jets with the anti-k_{T} jet-algorithm [46], as implemented in the FASTJET package [47], with a distance parameter of R=0.4.

In the low $p_{\mathrm{T},Zj}$ region one can clearly see the expected steeply rising behavior of the fixed NLO prediction. In the $\Delta\phi_{\mathrm{Zj}}$ distribution one can observe the limited region for fixed NLO at $\Delta\phi_{\mathrm{Zj}} < 2/3\pi$, since at most two jets in addition to the Z boson appear in the calculation. At large $\Delta\phi_{\mathrm{Zj}}$, the fixed NLO prediction rises faster than the full calculation including resummation via PB-TMDs and parton showers. In the following we concentrate on the large $\Delta\phi_{\mathrm{Zj}}$ region.

3 Back-to-back azimuthal correlations in Z+jet and multijet production

We now present predictions, obtained in the framework described above, for Z+jet and multijet production.* The selection of events follows the one of azimuthal correlations $\Delta\phi_{12}$ in the back-to-back region ($\Delta\phi_{12} \to \pi$) in multijet production at $\sqrt{s} = 13$ TeV as obtained by CMS [5]: jets are reconstructed with the anti-k_{T} algorithm [46] with a distance parameter of 0.4 in the rapidity range of $|y| < 2.4$. We require either two jets with $p_{\mathrm{T}}^{\mathrm{leading}} > 200$ GeV or a Z boson and a jet as leading or subleading objects with a transverse momentum $p_{\mathrm{T}}^{\mathrm{leading}} > 200$ GeV.

We consider distributions of the azimuthal correlation between the Z boson and the leading jet, $\Delta\phi_{\mathrm{Zj}}$, for $p_{\mathrm{T}}^{\mathrm{leading}} > 200$ GeV as well as for the very high p_{T} region of $p_{\mathrm{T}}^{\mathrm{leading}} > 1000$ GeV.

The calculations are performed with MCatNLO+CAS3 using PB-NLO-2018-Set 2 as the collinear and TMD parton densities with running coupling satisfying $\alpha_{\mathrm{s}}(m_{\mathrm{Z}}) = 0.118$ and PB-TMD parton shower.

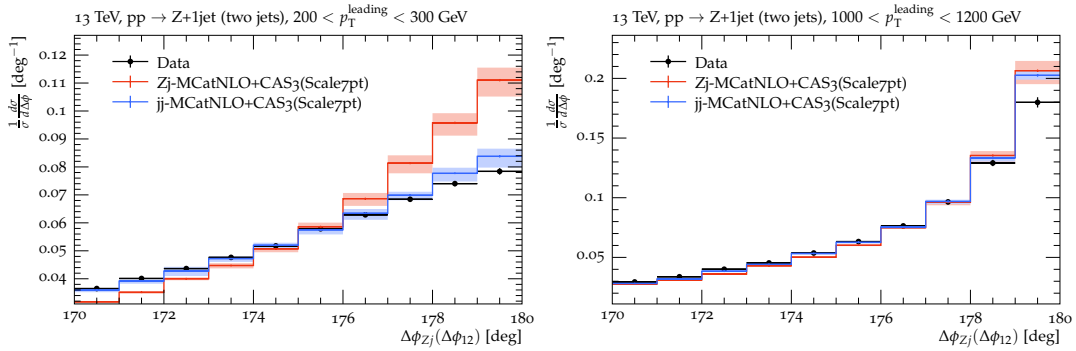

Figure 3: Predictions of the azimuthal correlation $\Delta\phi_{\mathrm{Zj}}(\Delta\phi_{12})$ for Z+jet and multijet processes in the back-to-back region for $p_{\mathrm{T}}^{\mathrm{leading}} > 200$ GeV (left) and $p_{\mathrm{T}}^{\mathrm{leading}} > 1000$ GeV (right) obtained from MCatNLO+CAS3. Shown are the uncertainties obtained from scale variation (as described in the text). The measurements of dijet correlations as obtained by CMS [5] are shown as data points, for comparison.

In Fig. 3, the prediction for the azimuthal correlations $\Delta\phi_{\mathrm{Zj}}$ for Z+jet production in the back-to-back region is shown.† We also show, for comparison, the prediction of azimuthal correlations $\Delta\phi_{12}$ for multijet production in the same kinematic region, compared to the measurement of dijet production obtained by CMS [5]. We observe that the distribution of

*A framework based on CCFM evolution [48] was described in [49, 50] for multi-jet and vector boson + jet correlations.

†Predictions for the region of small $\Delta\phi$ require including the contribution of higher parton multiplicities, e.g. via multi-jet merging [51].

azimuthal angle $\Delta\phi_{\mathrm{Zj}}$ in Z+jet-production for $p_{\mathrm{T}}^{\mathrm{leading}} > 200$ GeV is more strongly correlated towards π than the distribution of angle $\Delta\phi_{12}$ in multijet production. This difference is reduced for $p_{\mathrm{T}}^{\mathrm{leading}} > 1000$ GeV.

Differences in $\Delta\phi$ between Z+jet and multijet production can result from the different flavor composition of the initial state and therefore different initial state transverse momenta and initial state parton shower, as well as from differences in final state showering since both processes have a different number of colored final state partons. Effects coming from factorization - breaking, interference between initial and final state partons, will depend on the final state structure and the number of colored final state partons.

We first investigate the role of initial state radiation and the dependence on the transverse momentum distributions coming from the TMD PDFs, which gives a large contribution to the decorrelation in $\Delta\phi$. The k_{T}-distribution obtained from a gluon TMD PDF is different from the one of a quark TMD PDF as shown in Fig. 1 for $x = 0.01$ and scales of $\mu = 200(1000)$ GeV. In Fig. 4 we show the probability of gg, qg and qq initial states (q stands for quark and antiquark) as a function of $p_{\mathrm{T}}^{\mathrm{leading}}$ for Z+jet and multijet production obtained with MCatNLO+CAS3. At high $p_{\mathrm{T}}^{\mathrm{leading}} > 1000$ GeV the qq channel becomes important for both Z+jet and multijet final states, while at lower $p_{\mathrm{T}}^{\mathrm{leading}} > 200$ GeV the gg channel is dominant in multijet production, leading to larger decorrelation effects, since gluons radiate more compared to quarks.

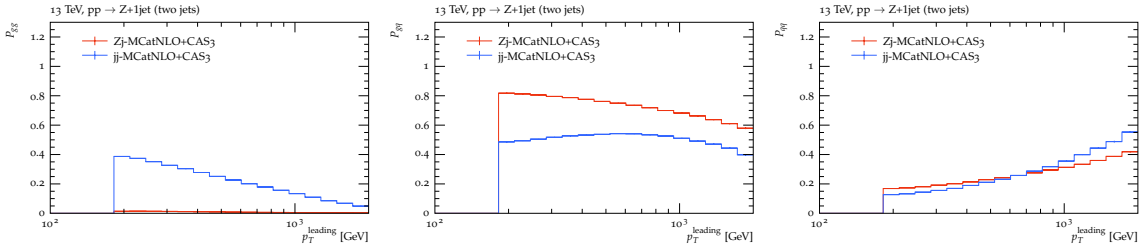

Figure 4: The probability of gg, qg and qq initial states in Z+jet and multijet production (q stands for quark and antiquark) as a function of $p_{\mathrm{T}}^{\mathrm{leading}}$. The predictions are calculated with MCatNLO+CAS3.

The role of final state radiation in the correlation in $\Delta\phi_{12}$ distributions is more difficult to estimate, since the subtraction terms for the NLO matrix element calculation also depend on the structure of the final state parton shower. In order to estimate the effect of final state shower we compare a calculation of the azimuthal correlations in the back-to-back region obtained with MCatNLO+CAS3 with the one obtained with MCatNLO+PYTHIA8 (Fig. 5). For the calculation MCatNLO+PYTHIA8 we apply the PYTHIA8 subtraction terms in the MADGRAPH5_AMC@NLO calculation, use the NNPDF3.0 [52] parton density and tune CUETP8M1 [53].

As shown in Fig. 5, the distributions are different because of the different parton shower in CASCADE3 and PYTHIA8, but the ratio of the distributions for Z+jet and multijet produc-

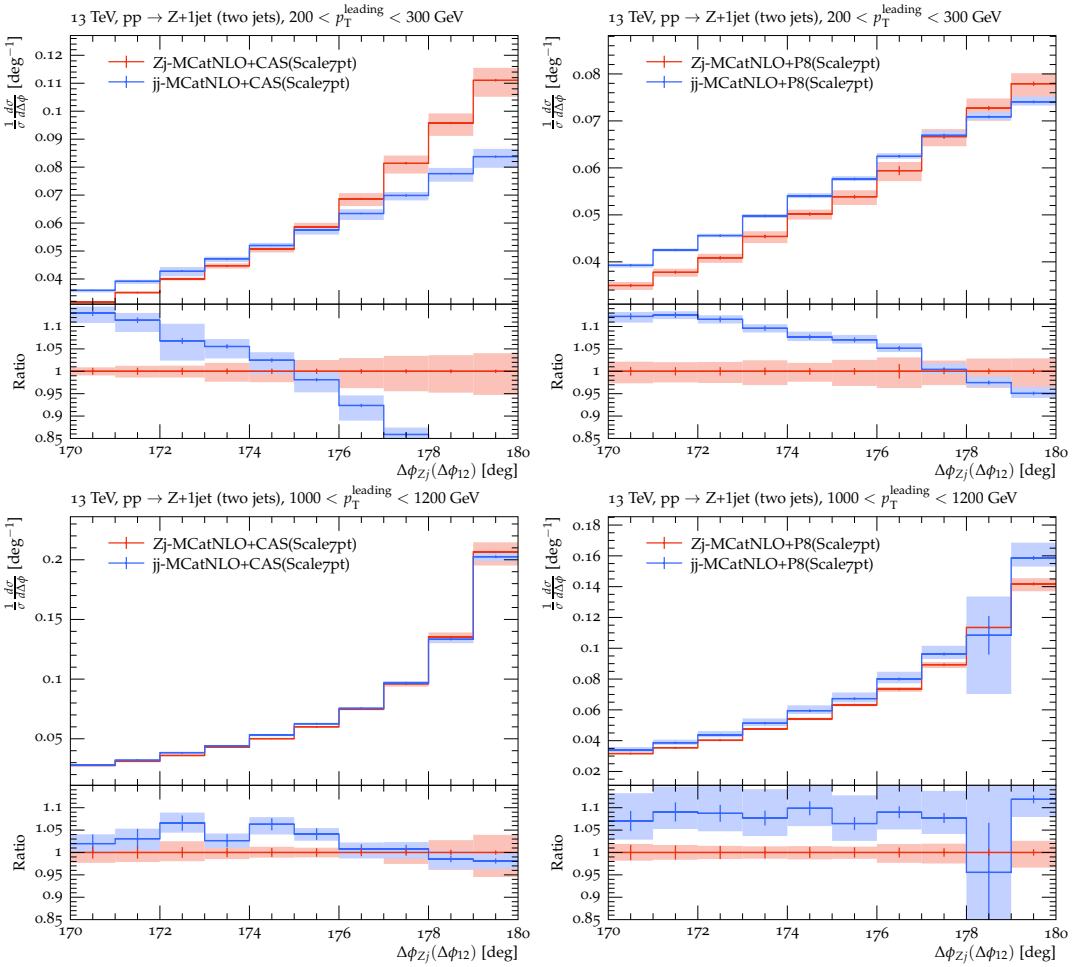

Figure 5: Predictions for the azimuthal correlation $\Delta\phi_{\mathrm{Zj}}(\Delta\phi_{12})$ in the back-to-back region for Z+jet and multijet production obtained with MCatNLO+CAS3 (left column) and MCatNLO+PYTHIA8 (right column). Shown are different regions in $p_{\mathrm{T}}^{\mathrm{leading}} > 200$ GeV (upper row) and $p_{\mathrm{T}}^{\mathrm{leading}} > 1000$ GeV (lower row). The bands show the uncertainties obtained from scale variation (as described in the text).

tion are similar: Z+jet-production gives a steeper (more strongly correlated) distribution at low $p_{\mathrm{T}}^{\mathrm{leading}}$, while at high $p_{\mathrm{T}}^{\mathrm{leading}}$ the distributions become similar in shape. We conclude, that the main effect of the $\Delta\phi$ decorrelation comes from initial state radiation, and the shape of the $\Delta\phi$ decorrelation in the back-to-back region becomes similar between Z+jet and dijet processes at high $p_{\mathrm{T}}^{\mathrm{leading}}$ where similar initial partonic states are important.

The matching scale μ_m limits the hardness of parton-shower emissions, and is thus typically a non-negligible source of variation in matched calculations (see e.g. [54] for a detailed

discussion). It is thus interesting to assess the robustness of the previous findings under variations of the matching scale. Assessing matching scale variations in both an angular-ordered shower – such as CASCADE3 – and a transverse-momentum-ordered shower – such as PYTHIA8 – additionally tests the *interpretation* of the matching scale. In transverse-momentum ordered showers, the matching scale sets the maximal transverse momentum of the first shower branchings, while branchings beyond the first emission are not explicitly affected by the matching scale. In an angular-ordered shower, however, the matching scale is applied as "veto scale" to avoid larger transverse momenta for any branching, i.e. the matching scale directly affects all branchings. The result of changing the matching scale to half or twice the central value is shown in Fig. 6. As expected, the value of the matching scale has an impact on the prediction ($\sim 5\%$). This is particularly apparent when μ_m is used to set the maximal transverse momentum of the first emission in PYTHIA8. Overall, we find that interpreting the matching scale as veto scale in CASCADE3 leads to apparently more robust predictions. Interestingly, the matching scale uncertainty becomes smaller for higher-$p_{\mathrm{T}}^{\mathrm{leading}}$ jet configurations in CASCADE3. The size of the matching scale variation is comparable to scale variations, and should thus be carefully studied when designing uncertainty estimates.

In dijet production the measurements are rather well described with predictions obtained with MCatNLO+CAS3, as shown in Fig. 3 and discussed in detail in Ref. [18]. Only in the very high $p_{\mathrm{T}}^{\mathrm{leading}}$ region, a deviation from the measurement is observed, which could be perhaps interpreted as coming from a violation of factorization. It is therefore very important to measure $\Delta\phi$ distributions in other processes, where factorization is expected to hold.

In order to experimentally probe effects which could originate from factorization - breaking in the back-to-back region we propose to measure the ratio of distributions in $\Delta\phi_{\mathrm{Zj}}$ for Z+jet and $\Delta\phi_{12}$ for multijet production at low and very high $p_{\mathrm{T}}^{\mathrm{leading}}$, and compare the measurement with predictions assuming that factorization holds. The number of colored partons involved in Z+jet and multijet events is different, and deviations from factorization will depend on the structure of the colored initial and final state. In order to minimize the effect of different initial state configurations, a measurement at high $p_{\mathrm{T}}^{\mathrm{leading}}$, could hint more clearly possible factorization - breaking effects.

4 Summary and conclusions

We have investigated azimuthal correlations in Z+jet production and compared predictions with those for multijet production in the same kinematic range. The predictions are based on PB-TMD distributions with NLO calculations via MCatNLO supplemented by PB-TMD parton showers via CASCADE3. The azimuthal correlations $\Delta\phi_{\mathrm{Zj}}$, obtained in Z+jet production are steeper compared to those in multijet production ($\Delta\phi_{12}$) at transverse momenta $\mathcal{O}(100)$ GeV, while they become similar for very high transverse momenta, $\mathcal{O}(1000)$ GeV, which is a result of similar initial parton configuration of both processes.

In Z+jet production the color and spin structure of the partonic final state is different compared to the one in multijet production, and differences in the azimuthal correlation

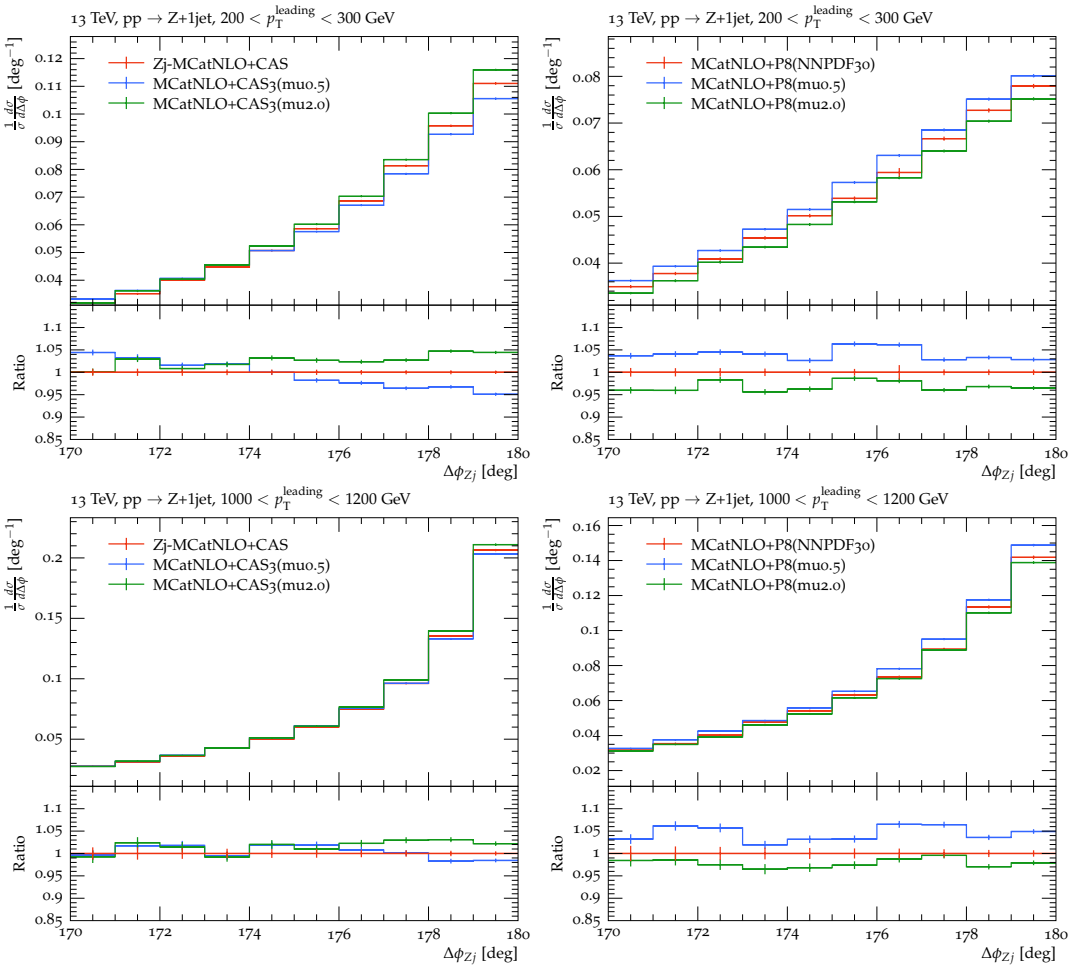

Figure 6: The dependence on the variation of the matching scale μ_m in predictions for the azimuthal correlation $\Delta\phi_{\mathrm{Zj}}(\Delta\phi_{12})$ in the back-to-back region. Shown are predictions obtained with MCatNLO+CAS3 (left column) and MCatNLO+PYTHIA8 (right column) for $p_{\mathrm{T}}^{\mathrm{leading}} > 200$ GeV (upper row) and $p_{\mathrm{T}}^{\mathrm{leading}} > 1000$ GeV (lower row). The predictions with different matching scales μ_m varied by a factor of two up and down are shown.

patterns can be used to search for potential factorization - breaking effects, involving initial and final state interferences. In order to experimentally investigate those effects, we propose to measure the ratio of the distributions in $\Delta\phi_{\mathrm{Zj}}$ for Z+jet- and $\Delta\phi_{12}$ for multijet production at low and at very high $p_{\mathrm{T}}^{\mathrm{leading}}$, and compare the measurements to predictions obtained assuming that factorization holds.

We have studied the matching scale dependence in the PB-TMD predictions and compared it with the case of NLO-matched calculations based on the PYTHIA8 collinear shower.

We find that variations of the matching scale lead to more stable predictions in the PB-TMD case, with the relative reduction of the matching scale theoretical uncertainty becoming more pronounced for increasing $p_{\mathrm{T}}^{\mathrm{leading}}$ transverse momenta.

Acknowledgments.
We are grateful to Olivier Mattelaer from the MADGRAPH5_AMC@NLO team for discussions, help and support with the lhe option for fixed NLO calculations in MCatNLO.

5 Appendix: Comparison of CASCADE3 and HERWIG6

Since HERWIG6 (H6) subtraction terms are used in the MCatNLO+CAS3 calculations, we investigate here in detail the contribution of the parton shower used in CASCADE3.

First we investigate final state parton showers. In CASCADE3, the PYTHIA6 final state shower is used (since the PB - method has not yet been applied for final state radiation), with the angular ordering veto condition. Since final state radiation is independent of parton densities, a direct comparison of MCatNLO+CAS3 and MCatNLO+H6, using the same LHE files, while only simulating final state radiation, is possible. In Fig. 7 we show a comparison of predictions for the transverse momentum of the first four jets in Z+jet events (using the LHE files used for the predictions in this paper). In H6 the allowed region of z for a branching $q \to qg$ in the shower is $Q_q/Q < z < 1 - Q_g/Q$ (e.g. A.2.2 in Ref. [55]), with $Q_q = m_q +$ `VQCUT` and $Q_g = m_g +$ `VGCUT`, and m_q, m_g being the quark and gluon effective masses, and `VQCUT,VGCUT` the minimum virtuality parameters. The uncertainty coming from different parameter settings in the H6 final state parton shower is estimated by changing the light quark masses from the default to 0.32 GeV(`Rmas = 0.32`, labelled as m_l) and `VQCUT,VGCUT` from the default to `VQCUT=VGCUT=0.1(1.5)`, labelled as $Vc_l(Vc_h)$, respectively. In Fig. 8 comparison is shown for the pseudorapidity η of the first four jets. Within the variation of the parameters, the prediction of MCatNLO+CAS3 agrees with the one of MCatNLO+H6, justifying the application of the PYTHIA6 final state parton shower algorithm.

Next we investigate the contribution of PB - TMD PDFs and the PB - TMD parton shower in the initial state and compare the predictions with the ones from H6. Since in H6 the initial state parton shower cannot be applied alone, but only in combination with the final state shower, we perform a similar calculation also with CASCADE3. In Fig. 9 we show a comparison of MCatNLO+CAS3 and MCatNLO+H6 predictions (including the same parameter variations for H6 as for the final state shower) for the transverse momentum of the first four jets. In Fig. 10 the corresponding comparison is shown for the pseudorapidity distributions. The transverse momentum distributions agree well within the uncertainties coming from parameter variations, while for the η-distributions some differences in the very forward/backward regions are seen. However, one can see, that a variation of `VQCUT,VGCUT` has an significant effect especially in the forward/backward region. Since these parameters are very different

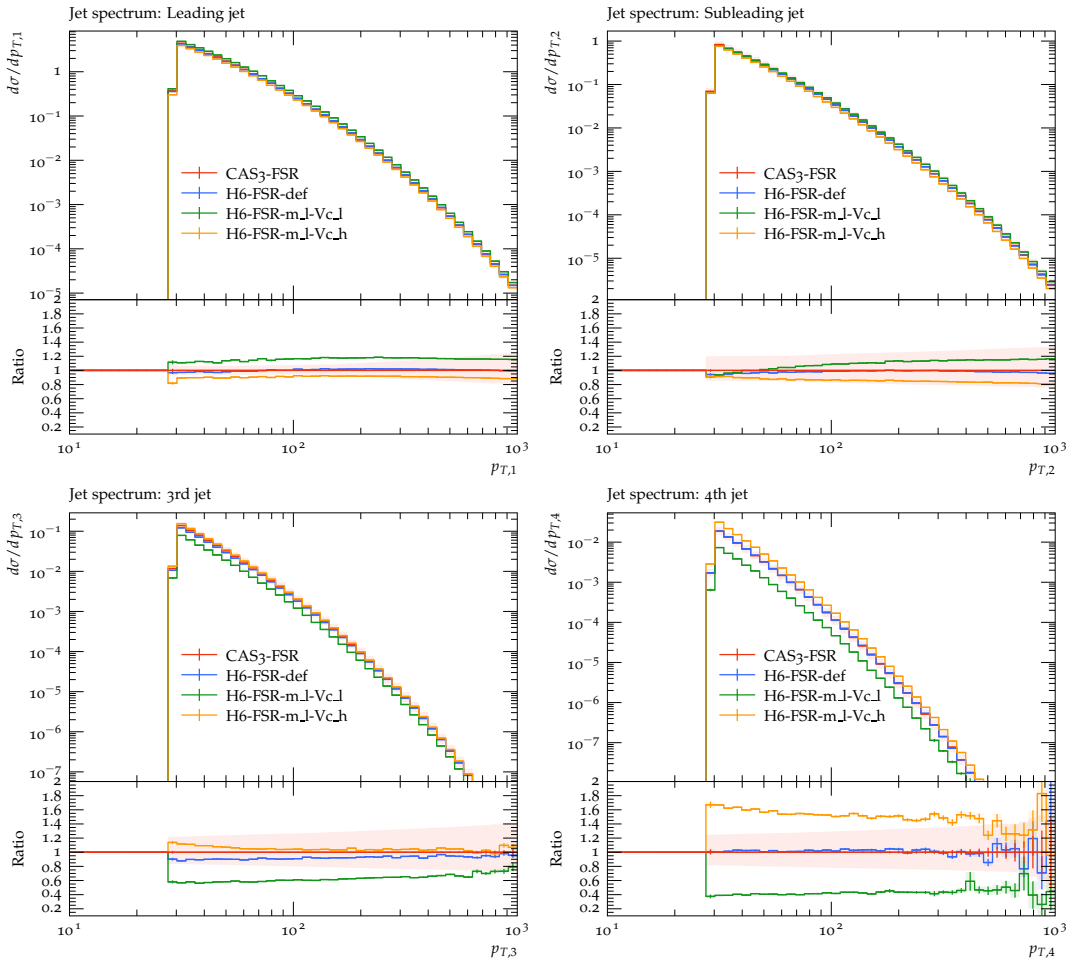

Figure 7: Comparison of predictions obtained with MCatNLO+CAS3 and MCatNLO+H6 for Z+jet obtained with MCatNLO. Shown are predictions using only final state parton shower. The band of MCatNLO+CAS3 shows the uncertainties obtained from scale variation (as described in the text).

from the ones used in PB TMD PDFs and the PB - TMD shower, we conclude that the use of H6 subtraction terms in MCatNLO is consistent with the use of PB - TMD PDFs, PB - TMD initial state parton shower, as applied in MCatNLO+CAS3.

References

[1] ATLAS Collaboration, "Measurement of dijet azimuthal decorrelations in pp collisions at sqrt(s)=7 TeV", *Phys.Rev.Lett.* **106** (2011) 172002, arXiv:1102.2696.

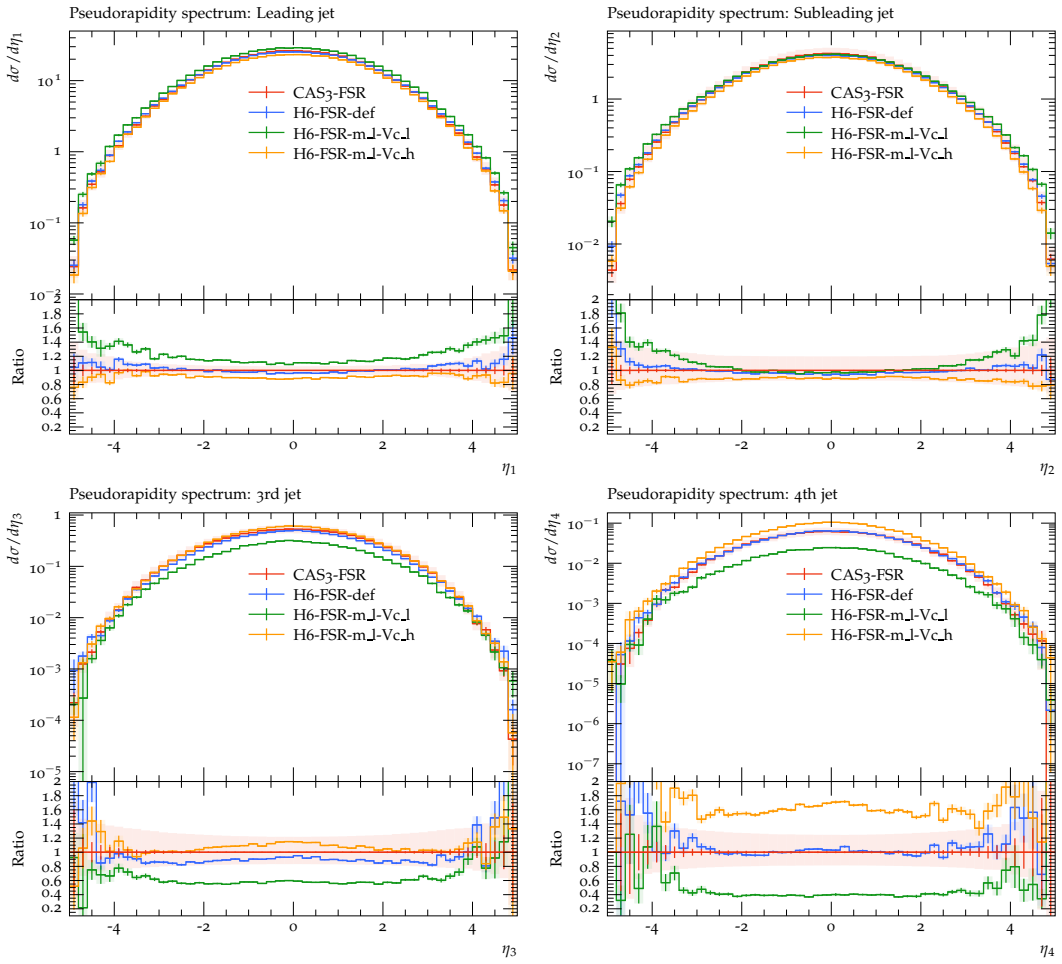

Figure 8: Comparison of predictions obtained with MCatNLO+CAS3 and MCatNLO+H6 for Z+jet obtained with MCatNLO. Shown are predictions using only final state parton shower. The band of MCatNLO+CAS3 show the uncertainties obtained from scale variation (as described in the text).

[2] CMS Collaboration, "Dijet Azimuthal Decorrelations in pp Collisions at sqrt(s) = 7 TeV", *Phys. Rev. Lett.* **106** (2011) 122003, arXiv:1101.5029.

[3] CMS Collaboration, "Measurement of dijet azimuthal decorrelation in pp collisions at $\sqrt{s} = 8\,\text{TeV}$", *Eur. Phys. J. C* **76** (2016) 536, arXiv:1602.04384.

[4] CMS Collaboration, "Azimuthal correlations for inclusive 2-jet, 3-jet, and 4-jet events in pp collisions at $\sqrt{s} = 13\,\text{TeV}$", *Eur. Phys. J.* **C78** (2018) 566, arXiv:1712.05471.

[5] CMS Collaboration, "Azimuthal separation in nearly back-to-back jet topologies in

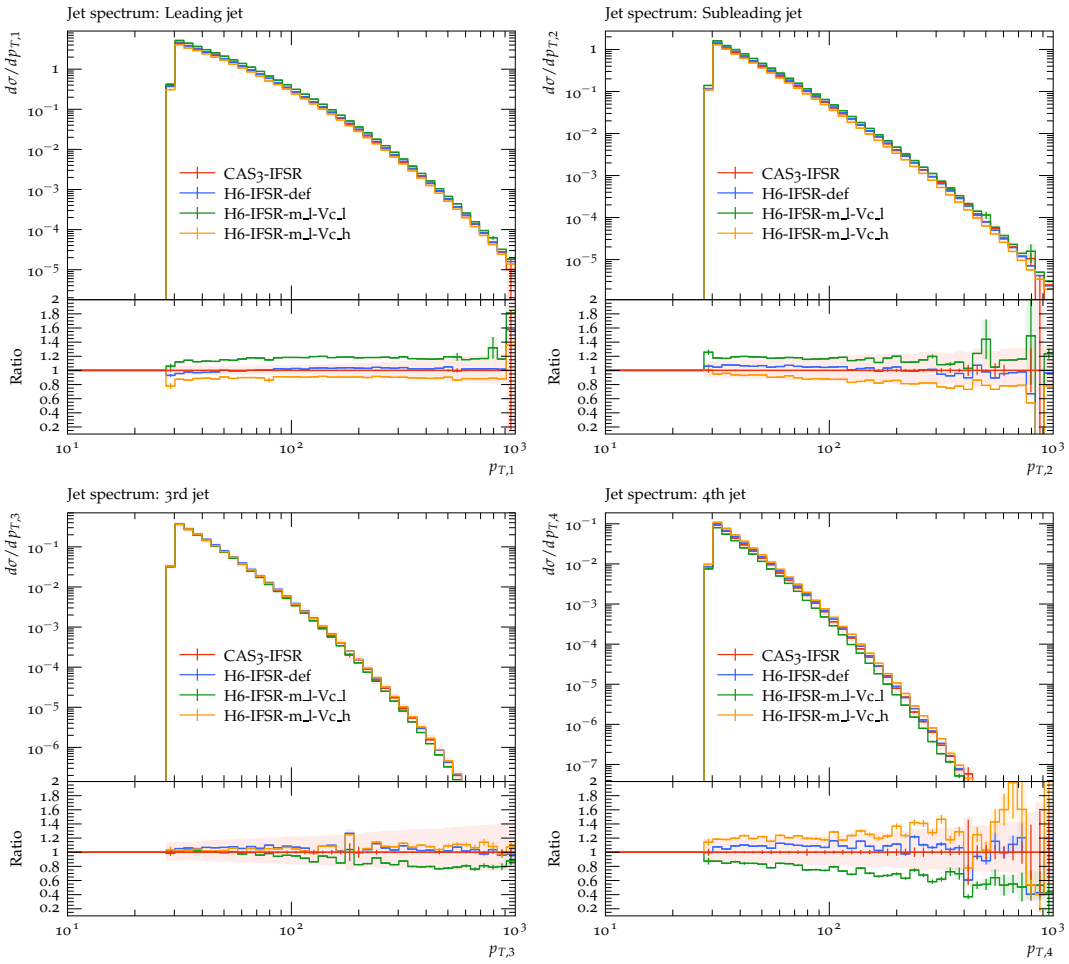

Figure 9: Comparison of predictions obtained with MCatNLO+CAS3 and MCatNLO+H6 for Z+jet obtained with MCatNLO. Shown are predictions using initial and final state parton shower. The band of MCatNLO+CAS3 show the uncertainties obtained from scale variation (as described in the text).

inclusive 2- and 3-jet events in pp collisions at $\sqrt{s} = 13$ TeV", *Eur. Phys. J. C* **79** (2019) 773, arXiv:1902.04374.

[6] CDF Collaboration, "Measurement of inclusive jet cross-sections in $Z/\gamma^* \to e^+e^-$ + jets production in $p\bar{p}$ collisions at $\sqrt{s}$ = 1.96-TeV", *Phys. Rev. Lett.* **100** (2008) 102001, arXiv:0711.3717.

[7] D0 Collaboration, "Measurement of differential Z/γ^* + jet + X cross sections in $p\bar{p}$ collisions at $\sqrt{s}$ = 1.96-TeV", *Phys. Lett.* **B669** (2008) 278–286, arXiv:0808.1296.

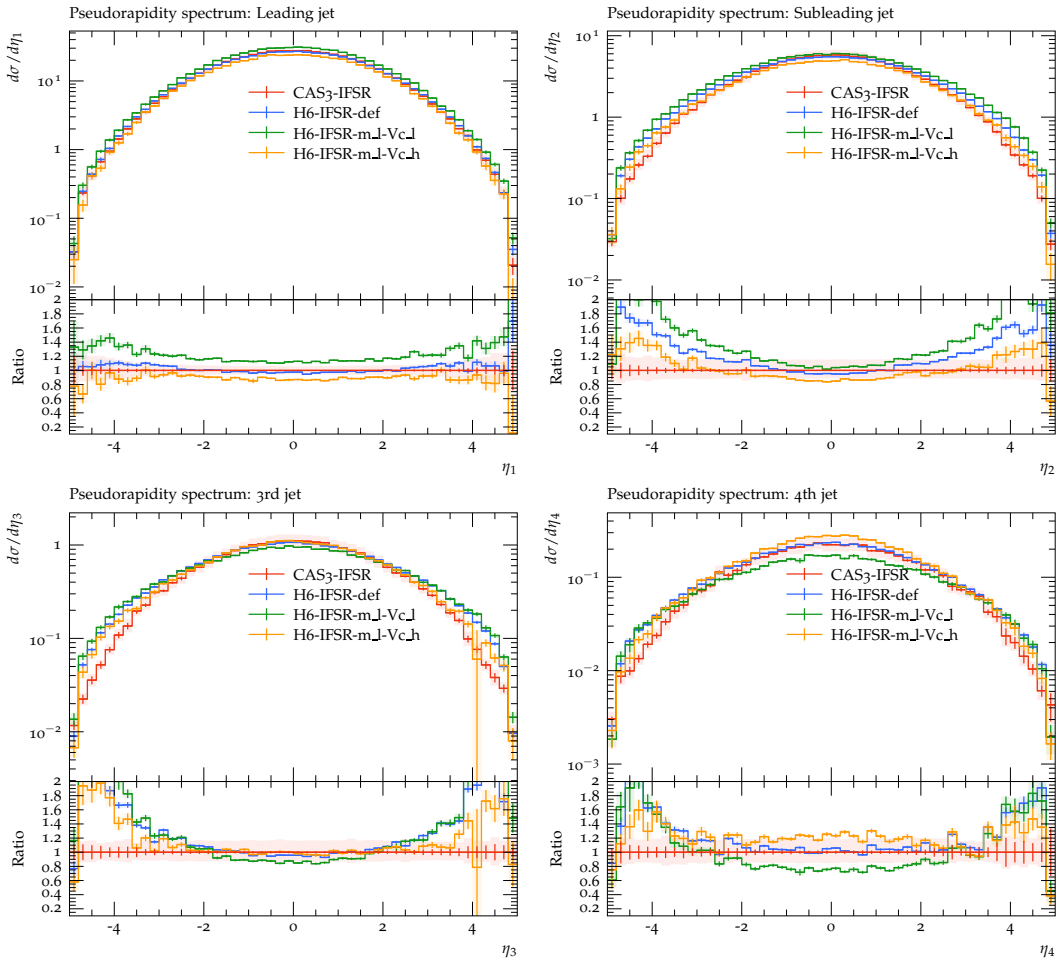

Figure 10: Comparison of predictions obtained with MCatNLO+CAS3 and MCatNLO+H6 for Z+jet obtained with MCatNLO. Shown are predictions using initial and final state parton shower. The band of MCatNLO+CAS3 show the uncertainties obtained from scale variation (as described in the text).

[8] ATLAS Collaboration, "Measurement of the production cross section of jets in association with a Z boson in pp collisions at $\sqrt{s}$ = 7 TeV with the ATLAS detector", *JHEP* **07** (2013) 032, arXiv:1304.7098.

[9] ATLAS Collaboration, "Measurement of the production cross section for Z/gamma* in association with jets in pp collisions at $\sqrt{s} = 7$ TeV with the ATLAS detector", *Phys. Rev. D* **85** (2012) 032009, arXiv:1111.2690.

[10] CMS Collaboration, "Measurements of jet multiplicity and differential production cross sections of $Z+$ jets events in proton-proton collisions at $\sqrt{s} = 7$ TeV", *Phys. Rev.*

D **91** (2015) 052008, arXiv:1408.3104.

[11] CMS Collaboration, "Measurements of differential production cross sections for a Z boson in association with jets in pp collisions at $\sqrt{s} = 8$ TeV", *JHEP* **04** (2017) 022, arXiv:1611.03844.

[12] ATLAS Collaboration, "Measurements of the production cross section of a Z boson in association with jets in pp collisions at $\sqrt{s} = 13$ TeV with the ATLAS detector", *Eur. Phys. J. C* **77** (2017) 361, arXiv:1702.05725.

[13] CMS Collaboration, "Measurement of differential cross sections for Z boson production in association with jets in proton-proton collisions at $\sqrt{s} = 13$ TeV", *Eur. Phys. J. C* **78** (2018) 965, arXiv:1804.05252.

[14] L. Buonocore, M. Grazzini, J. Haag, and L. Rottoli, "Transverse-momentum resummation for boson plus jet production at hadron colliders", *Eur. Phys. J. C* **82** (2022), no. 1, 27, arXiv:2110.06913.

[15] M. G. A. Buffing, Z.-B. Kang, K. Lee, and X. Liu, "A transverse momentum dependent framework for back-to-back photon+jet production", arXiv:1812.07549.

[16] Y.-T. Chien, D. Y. Shao, and B. Wu, "Resummation of Boson-Jet Correlation at Hadron Colliders", *JHEP* **11** (2019) 025, arXiv:1905.01335.

[17] P. Sun, B. Yan, C. P. Yuan, and F. Yuan, "Resummation of High Order Corrections in Z Boson Plus Jet Production at the LHC", *Phys. Rev. D* **100** (2019), no. 5, 054032, arXiv:1810.03804.

[18] M. I. Abdulhamid et al., "Azimuthal correlations of high transverse momentum jets at next-to-leading order in the parton branching method", *Eur. Phys. J. C* **82** (2022) 36, arXiv:2112.10465.

[19] R. Angeles-Martinez et al., "Transverse Momentum Dependent (TMD) parton distribution functions: status and prospects", *Acta Phys. Polon. B* **46** (2015), no. 12, 2501, arXiv:1507.05267.

[20] J. Collins and J.-W. Qiu, "k_T factorization is violated in production of high-transverse-momentum particles in hadron-hadron collisions", *Phys. Rev. D* **75** (2007) 114014, arXiv:0705.2141.

[21] W. Vogelsang and F. Yuan, "Hadronic Dijet Imbalance and Transverse-Momentum Dependent Parton Distributions", *Phys. Rev. D* **76** (2007) 094013, arXiv:0708.4398.

[22] T. C. Rogers and P. J. Mulders, "No Generalized TMD-Factorization in Hadro-Production of High Transverse Momentum Hadrons", *Phys.Rev.* **D81** (2010) 094006, arXiv:1001.2977.

[23] T. C. Rogers, "Extra spin asymmetries from the breakdown of transverse-momentum-dependent factorization in hadron-hadron collisions", *Phys. Rev. D* **88** (2013), no. 1, 014002, arXiv:1304.4251.

[24] Y.-T. Chien et al., "Precision boson-jet azimuthal decorrelation at hadron colliders", arXiv:2205.05104.

[25] F. Hautmann et al., "Soft-gluon resolution scale in QCD evolution equations", *Phys. Lett. B* **772** (2017) 446, arXiv:1704.01757.

[26] F. Hautmann et al., "Collinear and TMD quark and gluon densities from Parton Branching solution of QCD evolution equations", *JHEP* **01** (2018) 070, arXiv:1708.03279.

[27] J. Alwall et al., "The automated computation of tree-level and next-to-leading order differential cross sections, and their matching to parton shower simulations", *JHEP* **1407** (2014) 079, arXiv:1405.0301.

[28] V. N. Gribov and L. N. Lipatov, "Deep inelastic ep scattering in perturbation theory", *Sov. J. Nucl. Phys.* **15** (1972) 438. [Yad. Fiz.15,781(1972)].

[29] L. N. Lipatov, "The parton model and perturbation theory", *Sov. J. Nucl. Phys.* **20** (1975) 94. [Yad. Fiz.20,181(1974)].

[30] G. Altarelli and G. Parisi, "Asymptotic freedom in parton language", *Nucl. Phys. B* **126** (1977) 298.

[31] Y. L. Dokshitzer, "Calculation of the structure functions for Deep Inelastic Scattering and e^+e^- annihilation by perturbation theory in Quantum Chromodynamics.", *Sov. Phys. JETP* **46** (1977) 641. [Zh. Eksp. Teor. Fiz.73,1216(1977)].

[32] G. Marchesini and B. R. Webber, "Monte Carlo Simulation of General Hard Processes with Coherent QCD Radiation", *Nucl. Phys.* **B310** (1988) 461.

[33] S. Catani, B. R. Webber, and G. Marchesini, "QCD coherent branching and semiinclusive processes at large x", *Nucl. Phys.* **B349** (1991) 635–654.

[34] F. Hautmann, L. Keersmaekers, A. Lelek, and A. M. Van Kampen, "Dynamical resolution scale in transverse momentum distributions at the LHC", *Nucl. Phys. B* **949** (2019) 114795, arXiv:1908.08524.

[35] A. Bermudez Martinez et al., "Collinear and TMD parton densities from fits to precision DIS measurements in the parton branching method", *Phys. Rev. D* **99** (2019) 074008, arXiv:1804.11152.

[36] ZEUS, H1 Collaboration, "Combination of measurements of inclusive deep inelastic $e^{\pm}p$ scattering cross sections and QCD analysis of HERA data", *Eur. Phys. J. C* **75** (2015) 580, arXiv:1506.06042.

[37] A. Bassetto, M. Ciafaloni, and G. Marchesini, "Jet Structure and Infrared Sensitive Quantities in Perturbative QCD", *Phys. Rept.* **100** (1983) 201–272.

[38] Y. L. Dokshitzer, V. A. Khoze, S. I. Troian, and A. H. Mueller, "QCD Coherence in High-Energy Reactions", *Rev. Mod. Phys.* **60** (1988) 373.

[39] A. Bermudez Martinez et al., "The transverse momentum spectrum of low mass Drell–Yan production at next-to-leading order in the parton branching method", *Eur. Phys. J. C* **80** (2020) 598, arXiv:2001.06488.

[40] A. Bermudez Martinez et al., "Production of Z-bosons in the parton branching method", *Phys. Rev. D* **100** (2019) 074027, arXiv:1906.00919.

[41] A. Bermudez Martinez et al., "The transverse momentum spectrum of low mass Drell–Yan production at next-to-leading order in the parton branching method", *Eur. Phys. J. C* **80** (2020), no. 7, 598, arXiv:2001.06488.

[42] S. Baranov et al., "CASCADE3 A Monte Carlo event generator based on TMDs", *Eur. Phys. J. C* **81** (2021) 425, arXiv:2101.10221.

[43] J. Alwall et al., "A standard format for Les Houches event files", *Comput. Phys. Commun.* **176** (2007) 300, arXiv:hep-ph/0609017.

[44] G. Corcella et al., "HERWIG 6.5 release note", arXiv:hep-ph/0210213.

[45] G. Marchesini et al., "HERWIG: A Monte Carlo event generator for simulating hadron emission reactions with interfering gluons. Version 5.1 - April 1991", *Comput. Phys. Commun.* **67** (1992) 465.

[46] M. Cacciari, G. P. Salam, and G. Soyez, "The anti-k_t jet clustering algorithm", *JHEP* **04** (2008) 063, arXiv:0802.1189.

[47] M. Cacciari, G. P. Salam, and G. Soyez, "FastJet User Manual", *Eur. Phys. J. C* **72** (2012) 1896, arXiv:1111.6097.

[48] H. Jung et al., "The CCFM Monte Carlo generator CASCADE version 2.2.03", *Eur. Phys. J. C* **70** (2010) 1237, arXiv:1008.0152.

[49] S. Dooling, F. Hautmann, and H. Jung, "Hadroproduction of electroweak gauge boson plus jets and TMD parton density functions", *Phys. Lett.* **B736** (2014) 293, arXiv:1406.2994.

[50] F. Hautmann and H. Jung, "Angular correlations in multi-jet final states from kt-dependent parton showers", *JHEP* **10** (2008) 113, arXiv:0805.1049.

[51] A. Bermudez Martinez, F. Hautmann, and M. L. Mangano, "TMD evolution and multi-jet merging", *Phys. Lett. B* **822** (2021) 136700, arXiv:2107.01224.

[52] NNPDF Collaboration, "Parton distributions for the LHC Run II", *JHEP* **04** (2015) 040, arXiv:1410.8849.

[53] CMS Collaboration, "Event generator tunes obtained from underlying event and multiparton scattering measurements", *Eur. Phys. J. C* **76** (2016) 155, arXiv:1512.00815.

[54] J. Bellm et al., "Parton Shower Uncertainties with Herwig 7: Benchmarks at Leading Order", *Eur. Phys. J. C* **76** (2016) 665, arXiv:1605.01338.

[55] S. Frixione, P. Nason, and B. R. Webber, "Matching NLO QCD and parton showers in heavy flavour production", *JHEP* **08** (2003) 007, arXiv:hep-ph/0305252.